

Phase transitions of polariton condensate in 2D Dirac materials

Ki Hoon Lee,^{1,2} Changhee Lee,² Hongki Min,^{2,*} and Suk Bum Chung^{1,2,3,†}

¹Center for Correlated Electron Systems, Institute for Basic Science (IBS), Seoul National University, Seoul 08826, Korea

²Department of Physics and Astronomy, Seoul National University, Seoul 08826, Korea

³Department of Physics, University of Seoul, Seoul 02504, Korea

For the quantum well in an optical microcavity, the interplay of the Coulomb interaction and the electron-photon (e-ph) coupling can lead to the hybridizations of the exciton and the cavity photon known as polaritons, which can form the Bose-Einstein condensate above a threshold density. Additional physics due to the nontrivial Berry phase comes into play when the quantum well consists of the gapped two-dimensional (2D) Dirac material such as the transition metal dichalcogenide (TMDC) MoS₂ or WSe₂. Specifically, in forming the polariton, the e-ph coupling from the optical selection rule due to the Berry phase can compete against the Coulomb electron-electron (e-e) interaction. We find that this competition gives rise to a rich phase diagram for the polariton condensate involving both topological and symmetry breaking phase transitions, with the former giving rise to the quantum anomalous Hall and the quantum spin Hall phases.

Monolayers of TMDC, such as MoS₂ and WSe₂, have attracted widespread interest in recent years as a semiconductor analogue of graphene. Like graphene, they are atomically thin, 2D materials with high mobility [1], with the band extrema occurring at the Brillouin zone corners K and K' due to their D_{3h} crystalline symmetry. Most crucially, these band extrema can be described very well by the Dirac Hamiltonian, which allows us to associate the $\pm\pi$ -Berry phase with each valley, but with direct band gaps at K and K' [2] unlike graphene.

Given the band structure origin of the valley Berry phase, we may ask whether and how it may be affected by the e-e interaction and the e-ph coupling. It has been discussed recently that the superconductivity, the condensation of e-e pairs due to e-e interaction, of the doped TMDC is topologically non-trivial due to the valley Berry phase [3–5]. Therefore, given the weak screening of the Coulomb interaction and the consequent strong binding of electron-hole pairs, *i.e.* excitons, that is known to occur [6, 7] in TMDC, it is natural to ask whether the condensate of excitons can also be topologically non-trivial. Meanwhile, the π -Berry phase has a well-known effect on the e-ph coupling, namely the optical valley selection rule for the circularly polarized light [2, 8, 9]. The TMDC monolayers are most convenient to manipulate optically, possessing direct band gaps (~ 1.5 to 2 eV) lying within the visible spectrum [10, 11].

The above considerations motivate us to study the condensation of polaritons, emergent bosons from hybridizations of cavity photons and excitons. It is tunable by both the Coulomb e-e interaction and the e-ph coupling, the former for the exciton energetics and the latter for the photon-exciton hybridization. The recent years have seen increasing consensus that this condensation has been experimentally observed in various systems [12–14] with progresses underway for TMDC [15, 16]. The room temperature polariton condensation may be possible, due to an especially small polariton mass from light-matter coupling [17]. The finite lifetime of both cavity photons

and excitons means that the polaritons exist in quasi-equilibrium. Despite the quasi-equilibrium nature, in the case of the polariton lifetime much longer than the thermalization time, substantial evidences of superfluidity, such as vortex formation [18], Goldstone modes [19], and the Landau critical velocity [20], have been observed. In this Letter, we will show the π -Berry phase effects on the TMDC polariton condensate phase diagrams.

The polariton condensation in our gapped Dirac materials should be derived from the electrons with the Coulomb interaction coupled to coherent photons. Hence the Hamiltonian we consider would be

$$\begin{aligned}\hat{H} &= \hat{H}_0 + \hat{H}_{e-e} + \hat{H}_{ph} + \hat{H}_{e-ph} - \mu_X \hat{N}_{tot}, \\ \hat{H}_0 &= \sum_{\tau=\pm} \sum_{\mathbf{k}} \left[\hat{c}_{\tau,1,\mathbf{k}}^\dagger \hat{c}_{\tau,2,\mathbf{k}}^\dagger \right] \mathbf{d}_{\tau}^{(0)}(\mathbf{k}) \cdot \boldsymbol{\sigma} \left[\hat{c}_{\tau,1,\mathbf{k}} \right], \\ \hat{H}_{ph} &= \hbar\omega_c \sum_I \left(\hat{a}_I^\dagger \hat{a}_I + \frac{1}{2} \right), \\ \hat{H}_{e-ph} &= -\frac{1}{c} \hat{\mathbf{A}} \cdot \sum_{\tau=\pm} \sum_{\mathbf{k}} \sum_{i,j} \mathbf{J}_{ij}^{\tau}(\mathbf{k}) \hat{c}_{\tau,i,\mathbf{k}}^\dagger \hat{c}_{\tau,j,\mathbf{k}}, \\ \hat{H}_{e-e} &= \frac{1}{2S} \sum_{\tau,\tau'} \sum_{\mathbf{k}_1,\mathbf{k}_2,\mathbf{q}} \sum_{i,j} V(\mathbf{q}) \hat{c}_{\tau,i,\mathbf{k}_1-\mathbf{q}}^\dagger \hat{c}_{\tau',j,\mathbf{k}_2+\mathbf{q}}^\dagger \hat{c}_{\tau',j,\mathbf{k}_2} \hat{c}_{\tau,i,\mathbf{k}_1},\end{aligned}\tag{1}$$

where $\boldsymbol{\sigma}$ represent the Pauli matrices, I the photon polarization index, $\mathbf{d}_{\tau}^{(0)}(\mathbf{k}) \equiv (\tau\hbar v k_x, \hbar v k_y, E_{\text{gap}}/2)$, with $\tau = \pm$ being the valley index, ω_c the cavity photon frequency and $V(\mathbf{q}) = \frac{2\pi e^2}{\epsilon q}$ the Coulomb interaction, with ϵ being the dielectric constant; note that the exchange terms of the e-e interaction are in the orbital rather than the band basis [21–23]. Meanwhile, the first quantized current operator is given by $\mathbf{J}_{ij}^{\tau}(\mathbf{k}) = -e\partial_{\mathbf{k}}[\mathbf{d}_{\tau}^{(0)}(\mathbf{k}) \cdot \boldsymbol{\sigma}]_{ij}$ and the gauge field operator by $\hat{\mathbf{A}} = \sum_I \sqrt{2\pi c^2 \hbar / \epsilon S L_c \omega_c} (\mathbf{e}_I \hat{a}_I e^{-i\omega_c t} + \mathbf{e}_I^* \hat{a}_I^\dagger e^{i\omega_c t})$, where \mathbf{e}_I is the photon polarization vector and S, L_c the cavity area and length, respectively. $\hat{c}_{1(2)}$ and \hat{a}_I are the annihilation operators for the electron in the $L_z = 0$ ($L_z = 2\tau$) orbital and the photon with the polarization I , respectively.

Each valley is taken to be completely spin-polarized with opposite spin polarization, *i.e.* $S_z = \tau/2$, due to the transition metal atomic spin-orbit coupling $\mathbf{L} \cdot \mathbf{S}$ removing the spin degeneracy in the $L_z = 2\tau$ orbital, and no intravalley spin-flip process is considered; hence, the dark excitons from intravalley spin-flip [24] will not be considered. Lastly, $\hat{N}_{\text{tot}} = \sum_I \hat{a}_I^\dagger \hat{a}_I + \hat{N}_{\text{ex}}$ is the total number of excitations, both photons and excitons, in the system and tuned by the chemical potential μ_X . Since the number of exciton \hat{N}_{ex} is the number of electrons excited from the valence band to the conduction band, the band basis for the electrons, $\sum_\alpha [W(\mathbf{k})]_{i,\alpha} \hat{\psi}_{\alpha,\mathbf{k}} = \hat{c}_{i,\mathbf{k}}$ which diagonalizes \hat{H}_0 of Eq. (1) with $\hat{\psi}_{c(v)}$ as the annihilation operator of electrons in the conduction (valence) band, can be convenient. This allows to identify the exciton number as $\hat{N}_{\text{ex}} \equiv \sum_{\tau,\mathbf{k}} \hat{n}_{\text{ex},\mathbf{k}}^\tau$ where $\hat{n}_{\text{ex},\mathbf{k}}^\tau \equiv (\hat{\psi}_{\tau,c,\mathbf{k}}^\dagger \hat{\psi}_{\tau,c,\mathbf{k}} + \hat{\psi}_{\tau,v,\mathbf{k}}^\dagger \hat{\psi}_{\tau,v,\mathbf{k}})/2$. Physically, we are interested in the thermal quasi-equilibrium that is reached after the cooling of a population of hot polaritons initially introduced by a short laser pulse [25]. For simplicity, we shall set the temperature to be zero.

We use the BCS variational wave function for the polariton condensate [22, 23]

$$|\Psi\{\Lambda_\pm\}\rangle = \mathcal{N} \prod_{I,\tau=\pm,\mathbf{k}} e^{\Lambda_I \hat{a}_I^\dagger} (u_{\tau,\mathbf{k}} + v_{\tau,\mathbf{k}} \hat{\psi}_{\tau,c,\mathbf{k}}^\dagger \hat{\psi}_{\tau,v,\mathbf{k}}) |0\rangle \quad (2)$$

with $\mathcal{N} = e^{-\sum_{I=\pm} \Lambda_I^2/2}$ and $|u_{\tau,\mathbf{k}}|^2 + |v_{\tau,\mathbf{k}}|^2 = 1$, where $I = \pm$ corresponds to the right (left) circular polarization $\mathbf{e}_\pm = (1, \pm i)/\sqrt{2}$ and $|0\rangle$ is the ground state of \hat{H}_0 , in which photons are absent and all the valence (conduction) band states are occupied (vacant). In this wave function, the photon component gives the coherent state with the number of photons $\langle \hat{a}_I^\dagger \hat{a}_I \rangle = \Lambda_I^2$ and of excitons $\langle \hat{N}_{\text{ex}} \rangle = \sum_{\mathbf{k}} |v_{\tau,\mathbf{k}}|^2$. To determine $\Lambda_\pm, u_{\tau,\mathbf{k}}, v_{\tau,\mathbf{k}}$ that minimize $\langle \Psi\{\Lambda_\pm\} | \hat{H} | \Psi\{\Lambda_\pm\} \rangle$, we obtain the mean-field self-consistency condition not only for the e-e interaction through $\hat{H}_{\text{e-e}}^{\text{MF}} = \sum_{\tau,i,j,\mathbf{k}} \tilde{\Delta}_{\tau;ij}(\mathbf{k}) \hat{c}_{\tau,i,\mathbf{k}}^\dagger \hat{c}_{\tau,j,\mathbf{k}}$ where [26]

$$\tilde{\Delta}_{\tau;ij}(\mathbf{k}) = -\frac{1}{S} \sum_{\mathbf{p}} V(\mathbf{k}-\mathbf{p}) \left\langle \hat{c}_{\tau,j,\mathbf{p}}^\dagger \hat{c}_{\tau,i,\mathbf{p}} \right\rangle_{\mu_X, \Lambda_\tau}^{\mu_X, \Lambda_\tau}, \quad (3)$$

but also for $\hat{H}_{\text{ph}} + \hat{H}_{\text{e-ph}}$, by which Λ_I 's are determined. To obtain the latter condition, we apply rotating wave approximation on e-ph coupling $\hat{H}_{\text{e-ph}} = \frac{1}{\sqrt{S}} \sum_{\mathbf{k}, I, \tau} g_{\mathbf{k}}^{I,\tau} \hat{a}_I \hat{\psi}_{\tau,c,\mathbf{k}}^\dagger \hat{\psi}_{\tau,v,\mathbf{k}} + \text{h.c.}$, where $g_{\mathbf{k}}^{I,\tau} = \sqrt{\frac{\hbar^3}{2\omega_c \epsilon S L_c}} \langle c | \mathbf{e}_I \cdot \mathbf{J}^{(\tau)}(\mathbf{k}) | v \rangle$ is the e-ph strength, which gives us [23]

$$\Lambda_I = -\frac{1}{\hbar\omega_c - \mu_X} \frac{1}{\sqrt{S}} \sum_{\tau,\mathbf{k}} \left(g_{\mathbf{k}}^{I,\tau} \right)^* \langle \hat{\psi}_{\tau,v,\mathbf{k}}^\dagger \hat{\psi}_{\tau,c,\mathbf{k}} \rangle. \quad (4)$$

The optical valley selection rule [2] gives us the *s*-wave symmetry for the e-ph coupling, *i.e.* $g_{\mathbf{k}}^{I,\tau} = g_0 \delta_{I,\tau} + O(k^2)$, where I is the photon circular polarization index.

From the self-consistency conditions of Eqs. (3) and (4), we find that there exists the competition between the e-e interaction and the e-ph coupling in the polariton condensation in the Dirac material. We first note that, the absorption of the right (left) circularly polarized photon creates the *s*-wave, *i.e.* isotropic, exciton at the \pm valley, as Λ_I in Eq. (4) is maximized when the e-ph coupling $g_{\mathbf{k}}^{I,\tau}$ and the exciton correlation $\langle \hat{\psi}_{\tau,c,\mathbf{k}}^\dagger \hat{\psi}_{\tau,v,\mathbf{k}} \rangle$ are in the same symmetry. On the other hand, the e-e interaction may not favor the *s*-wave exciton when we examine $\hat{H}_{\text{e-e}}^{\text{MF}} = \sum_{\tau,\alpha,\beta,\mathbf{k}} \Delta_{\tau;\beta\alpha}(\mathbf{k}) \hat{\psi}_{\tau,\beta,\mathbf{k}}^\dagger \hat{\psi}_{\tau,\alpha,\mathbf{k}}$, given that

$$\begin{aligned} \Delta_{\tau;c,v}(\mathbf{k}) &= \sum_{i,j} [W \tilde{\Delta} W^\dagger]_{\tau;c,v}(\mathbf{k}) \approx \Delta_{\tau;c,v}^s(k) + e^{i\tau\phi_{\mathbf{k}}} \Delta_{\tau;c,v}^p(k), \\ \Delta_{\tau;c,v}^s(k) &\approx -\frac{1}{S} \cos^2 \frac{\theta_k}{2} \sum_{\mathbf{p}} V(|\mathbf{k}-\mathbf{p}|) \langle \hat{\psi}_{\tau,v,\mathbf{p}}^\dagger \hat{\psi}_{\tau,c,\mathbf{p}} \rangle \cos^2 \frac{\theta_p}{2}, \\ \Delta_{\tau;c,v}^p(k) &\approx -\frac{2}{S} \sin \theta_k \sum_{\mathbf{p}} V(|\mathbf{k}-\mathbf{p}|) \langle \hat{n}_{\text{ex},\mathbf{p}}^\tau \rangle \cos \theta_p, \end{aligned} \quad (5)$$

where $\tan \phi_{\mathbf{k}} \equiv k_y/k_x$, $\tan \theta_k \equiv \hbar v k / (E_{\text{gap}}/2)$. The *p*-wave components $\Delta_{\tau;c,v}^p(k)$ arises from the $\tau\pi$ Berry phase, as can be seen both from the chiralities of the *p*-wave components for the two valleys being opposite and $\Delta_{\tau;c,v}^p(k)$ being proportional to $\sin \theta_k$, the integrated Berry curvature for momenta smaller than k , that vanishes linearly as $k \rightarrow 0$. We see from Eq. (5) that the Coulomb e-e interaction favors the *p*-wave (*s*-wave) exciton at the τ valley when the τ -valley exciton density $\sum_{\mathbf{p}} \langle \hat{n}_{\text{ex},\mathbf{p}}^\tau \rangle$ becomes sufficiently large (small) compared to the critical density set by the average Berry curvature. We will show that when the exciton symmetry of the polariton condensate is predominantly chiral *p*-wave in the τ valley, the Berry phase sign of τ valley changes in the mean-field Hamiltonian $\hat{H}^{\text{MF}} \equiv \hat{H}_0 + \frac{1}{\sqrt{S}} \sum_{I,\tau,\mathbf{k}} (\Lambda_I g_{\mathbf{k}}^{I,\tau} \hat{\psi}_{\tau,c,\mathbf{k}}^\dagger \hat{\psi}_{\tau,v,\mathbf{k}} + \text{h.c.}) + \hat{H}_{\text{e-e}}^{\text{MF}} - \mu_X \hat{N}_{\text{ex}}$ from that of \hat{H}_0 . While Eq. (5) also indicates that the chiral *p*-wave excitons are due to a component of the e-e interaction that violates the N_{tot} conservation, the N_{tot} fluctuation remains small, *i.e.* $\frac{\langle (\Delta \hat{N}_{\text{tot}})^2 \rangle}{N_{\text{tot}}^2} = \frac{\Lambda^2 + \sum_{\mathbf{k}} |u_{\mathbf{k}}|^2 |v_{\mathbf{k}}|^2}{(\Lambda^2 + \sum_{\mathbf{k}} |v_{\mathbf{k}}|^2)^2} \ll 1$.

The essence of the competition between the e-e interaction and the e-ph coupling can emerge clearly from considering only a single valley, *i.e.* the $\tau = -$ valley coupled to the $I = -$ photons, revealing how the competition can give rise to the phase transition of our polariton condensate. Fig. 1(a) shows how the photon fraction $\Lambda^2/(\Lambda^2 + \langle \hat{N}_{\text{ex}} \rangle)$ of the polariton condensate and the exciton gap parameters $\Delta^{s,p}$ of Eq.(5) depend on the mean distance R_s between excitations, the quantity that determines the total number of excitations N_{tot} . A key feature here is that the *p*-wave excitons are dark [27], which can be confirmed from Λ vanishing in Eq.(4) for the purely *p*-wave $\langle \hat{\psi}_v^\dagger \hat{\psi}_c \rangle$ because the *s*-wave symmetry for the e-ph coupling, *i.e.* $g_{\mathbf{k}} \approx g_0 \delta_{I,\tau}$. Since Δ^p arises solely from the e-e interaction, the higher-density discontinuous crossing

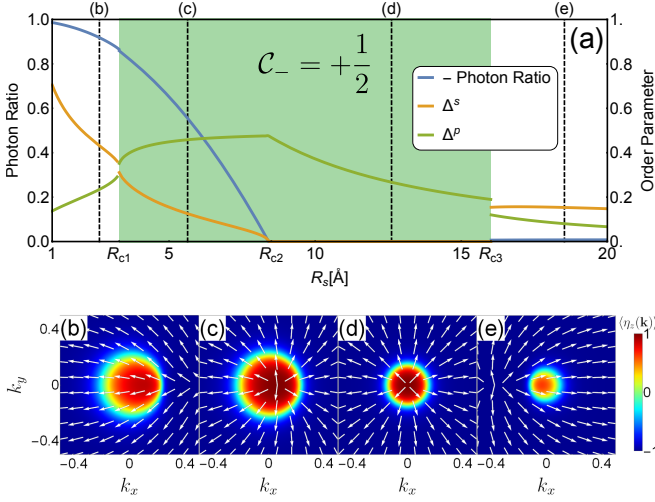


FIG. 1. (a) Photon fraction and mean-field band exciton gap parameters $\Delta^{s,p}$ averaged over the momentum space as the functions of R_s for the photon frequency $\hbar\omega_c = 2.1$ eV, the dielectric constant $\epsilon = 10$, the Dirac velocity $\hbar v = 3.7$ eVÅ, and the band gap of $E_{\text{gap}} = 2.0$ eV. (b)-(e) Pseudo-spin textures at the R_s values indicated in (a). Arrow represents $\hat{\eta}_{\parallel}$ and false color represents $\eta_z(\mathbf{k})$; for convenience, we have plotted the $\tau = -$ valley coupled to $I = -$ photons.

of $|\Delta^s|$ and $|\Delta^p|$ curves in Fig. 1(a) at $R_s = R_{c1}$ can be regarded as a consequence of the competition between the e-e interaction and the e-ph coupling.

The lower density transition in Fig. 1(a) at $R_s = R_{c3}$ involves little e-ph coupling, and can be attributed to the competition between different components of the e-e interactions shown in Eq.(5), which favors the chiral p -wave exciton for the large $\sum_{\mathbf{k}} \langle \hat{n}_{\text{ex},\mathbf{k}}^{\tau} \rangle$ (or small R_s) and the s -wave exciton for the small $\sum_{\mathbf{k}} \langle \hat{n}_{\text{ex},\mathbf{k}}^{\tau} \rangle$ (or large R_s). As shown in Fig. 1(b)-(e), the transitions at both $R_s = R_{c1}$ and $R_s = R_{c3}$ can be illustrated using the pseudo-spin texture defined from the parametrization of the mean-field Hamiltonian: $\sum_{\mathbf{k},\alpha,\beta} \hat{\psi}_{\alpha,\mathbf{k}}^{\dagger} [\boldsymbol{\sigma} \cdot \boldsymbol{\eta}(\mathbf{k})]_{\alpha\beta} \hat{\psi}_{\beta,\mathbf{k}} \equiv \hat{H}^{\text{MF}}$. One can see that both transitions involve the (dis)appearance of the skyrmion texture in the $\hat{\eta}$ configuration, which requires in the $\eta_z > 0$ region the singularity of $\hat{\eta}_{\parallel} \equiv \hat{\eta} - (\hat{\eta} \cdot \hat{\mathbf{z}})\hat{\mathbf{z}}$, while $\hat{\eta} = -\hat{\mathbf{z}}$ as $k \rightarrow \infty$. However, Fig. 1 (d) and (e) show that, for the $R_s = R_{c3}$ transition, the $\hat{\eta}_{\parallel}$ singularity jumps from $\mathbf{k} = 0$ to the $\eta_z < 0$ region, while for the $R_s = R_{c1}$ transition, the $\hat{\eta}_{\parallel}$ singularity jumps from the $\eta_z < 0$ region into the $\eta_z \gtrsim 0$ region away from $\mathbf{k} = 0$, nearly closing the quasiparticle energy gap. This implies that the topological phase transition at $R_s = R_{c3}$ also involves the changes in the exciton symmetry.

Overall, the Fig. 1 plots show how the topological phase transition of \hat{H}^{MF} can arise from the competition between the s -wave and the chiral p -wave exciton pairing channels. Note how the Chern number $\mathcal{C}_- = \pm \frac{1}{2}$ coincides exactly with $|\Delta^s| < |\Delta^p|$ ($|\Delta^s| > |\Delta^p|$) in

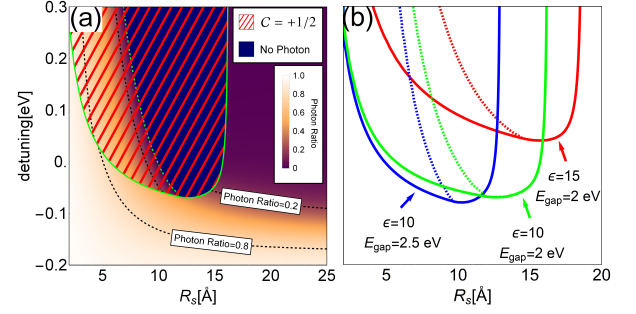


FIG. 2. (a) The dependence of photon fraction for the single-valley TMDC polariton system on δ and R_s shown with the velocity $\hbar v = 3.7$ eVÅ, the dielectric constant $\epsilon = 10$ and $E_{\text{gap}} = 2.0$ eV; the green solid, the green dashed and the black dotted curves represent the first-order transitions, the second-order transitions, and the crossovers, respectively. (b) Phase boundaries for the first-order (solid) and second-order (dashed) transitions for $\epsilon=10$ and $E_{\text{gap}}=2$ eV (green), $\epsilon=15$ and $E_{\text{gap}}=2$ eV (red), and $\epsilon=10$ and $E_{\text{gap}}=2.5$ eV (blue).

Fig. 1 (a). \mathcal{C}_- can be computed equivalently in either the orbital basis obtained from $\boldsymbol{\sigma} \cdot \hat{\mathbf{d}} = W(\boldsymbol{\sigma} \cdot \hat{\boldsymbol{\eta}})W^{\dagger}$ or the band basis as $\mathcal{C}_- = \frac{1}{4\pi} \int d^2k \hat{\mathbf{d}} \cdot (\partial_{k_x} \hat{\mathbf{d}} \times \partial_{k_y} \hat{\mathbf{d}}) = -\frac{1}{2} + \frac{1}{4\pi} \int d^2k \hat{\boldsymbol{\eta}} \cdot (\partial_{k_x} \hat{\boldsymbol{\eta}} \times \partial_{k_y} \hat{\boldsymbol{\eta}})$, which is consistent with Fig. 1 (b)-(e) as it gives $\mathcal{C}_- = \pm \frac{1}{2}$ when the skyrmion is present (absent); note that \hat{H}_0 gives $\mathcal{C}_- = -\frac{1}{2}$. In fact, we may define the overall exciton symmetry to be chiral p -wave when $\mathcal{C}_- = +\frac{1}{2}$. Given that the Δ^p arises from the non-conservation of N_{tot} as can be seen from Eq.(5), this is a case of discontinuous phase transitions to excitonic insulator phases in absence of the N_{tot} conservation, though our case deals with quantum rather than classical phase transitions considered in [28, 29].

The full phase diagrams with respect to R_s and the photon detuning $\delta \equiv \hbar\omega_c - E_{\text{gap}}$ shown as Fig. 2 for different values of the dielectric constant ϵ and the band gap E_{gap} can be largely explained by the different energy competitions that give rise to the higher and the lower density phase transition. δ and ϵ are control parameters in the competition between the e-ph coupling and the e-e interaction; the photon self-consistency equation Eq.(4) shows that the smaller δ leads to the larger photon fraction, while the smaller ϵ leads to the larger e-e interaction. Fig. 2 (b) shows that the $\mathcal{C}_- = +\frac{1}{2}$ phase with the chiral p -wave excitons requires sufficiently weak e-ph coupling, which is naturally larger for the smaller Coulomb interaction of $\epsilon = 15$ shown in red than for the larger Coulomb interaction of $\epsilon = 10$ shown in blue and green. That the lower density (larger R_s) transition depends little on δ confirms its weak dependence on the e-ph coupling. Meanwhile, the blue curves of Fig. 2 (b) shows that for a larger E_{gap} the lower density transition occurring at smaller R_s (larger density) when compared with the lower E_{gap} shown by the green and red curves. This is because of the larger E_{gap} suppressing Δ^p through re-

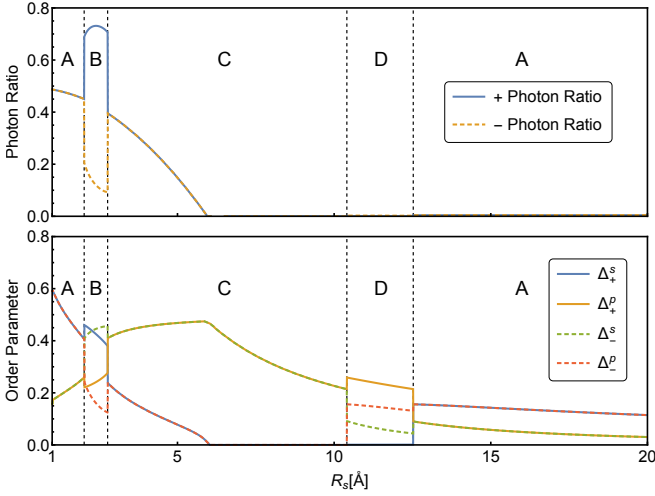


FIG. 3. Photon fraction (above) and mean-field band exciton gap parameters $\Delta^{s,p}$ (below) for two valleys ($\tau = \pm 1$) as the functions of R_s for the photon frequency $\hbar\omega_c = 2.1$ eV and other physical parameters following those of Fig. 2 (a).

ducing $\sin\theta_k$ at all momenta, or, equivalently, the Berry curvature integrated over momenta smaller than k .

The phase diagram of Fig. 2 (a) shows phase transitions as well as crossovers in contrast to the results for the polariton condensate in the topologically trivial quantum well where only the latter were present [22]. Following the results of Kamide *et al.* for the topologically trivial quantum well, we can define in the $\mathcal{C}_- = -\frac{1}{2}$ region several phases according to the photon fraction as the photon, the polariton and the exciton BEC in the decreasing order, with their boundaries being crossovers (shown as the dotted curves). However, as discussed above, there is a first-order phase transition (shown as the solid curves) between the $\mathcal{C}_- = -\frac{1}{2}$ and the $\mathcal{C}_- = +\frac{1}{2}$ regions. Within the $\mathcal{C}_- = +\frac{1}{2}$ region, the phase with the vanishing photon fraction would be best termed the electron-hole BCS condensate, with BCS indicating the exciton radius being larger than R_s . Inside the $\mathcal{C}_- = +\frac{1}{2}$ region, there is a second-order phase transition (shown as the dashed curves) between the polariton BEC and this electron-hole BCS condensate involving the spontaneous rotational symmetry breaking. Despite photons providing no preferred direction, the rotational symmetry is broken when we have both the s -wave and the chiral p -wave components in $v_{\mathbf{k}}/u_{\mathbf{k}}$ of the exciton wave function Eq.(2), which moves the singularity of η_{\parallel} textures of Fig. 1 (b), (c), (e) away from $\mathbf{k} = 0$. The rotational symmetry in our polariton condensate is restored in Fig. 1 (d) on Λ and Δ^s vanishing continuously. Hence our polariton condensate always possesses either topology or symmetry distinct from the ground state of \hat{H}_0 .

For the two valley TMDC coupled to photons of both circular polarizations shown in Fig. 3, we find that the topological phase transitions give rise to both the quan-

	$\mathcal{C}_{+\uparrow}$	$\mathcal{C}_{+\downarrow}$	$\mathcal{C}_{-\uparrow}$	$\mathcal{C}_{-\downarrow}$	\mathcal{C}_S	\mathcal{C}_V	\mathcal{C}_{tot}
A	+1/2	+1/2	-1/2	-1/2	0	+1	0
B	$\pm 1/2$	+1/2	-1/2	$\pm 1/2$	-1/2	+1/2	± 1
C	-1/2	+1/2	-1/2	+1/2	-1	0	0
D	$\mp 1/2$	+1/2	-1/2	$\mp 1/2$	-1/2	+1/2	∓ 1

TABLE I. Phase classification in the two valleys coupled to the photons of both circular polarizations. The alphabet letters in the leftmost column refer to each phase mentioned in Fig. 3. $\mathcal{C}_S \equiv \sum_{\tau,\sigma} \sigma \mathcal{C}_{\tau,\sigma}/2$ and $\mathcal{C}_V \equiv \sum_{\tau,\sigma} \tau \mathcal{C}_{\tau,\sigma}/2$ are the spin and the valley Chern numbers respectively. Refer the main text for further details.

tum spin Hall phase (in the region C) and the quantum anomalous Hall phase (in the regions B and D). To analyze this problem, we consider the variational solution of Eq. (2) with the phase difference between the two photon polarizations fixed. In the absence of interactions, \hat{H}_0 of Eq. (1) gives us the opposite sign for the Chern numbers of $\mathcal{C}_\tau = \frac{\tau}{2}$ for the τ valley. When the exciton symmetry of one valley is the chiral p -wave and that of the other valley is the s -wave, we have a net Chern number of $\mathcal{C}_{\text{tot}} \equiv \sum_{\tau,\sigma} \mathcal{C}_{\tau,\sigma} = \pm 1$ for our \hat{H}^{MF} and hence the quantum anomalous Hall phase [30]. Due to the valley polarization that occurs only in this phase, the regions B and D have the elliptic photon polarizations while all the other regions have the linear photon polarizations. Meanwhile, the region C of Fig. 3 shows that the photon fraction and the Δ^s at both valleys vanish continuously at the same R_s [31]. In the region C, we have the quantum spin Hall phase where the time-reversal symmetry is restored by the opposite chirality between the p -wave excitons of the two valleys. Table 1 shows the topological phases for the two-valley TMDC polariton condensate taking into account both spin components at each valley.

In summary, we have studied the quasi-equilibrium ground state of the TMDC monolayer coupled to the cavity photons with the self-consistent mean-field theory and found topological phase transitions due to the competition between the e-ph coupling and the e-e interaction tuned by the excitation density. Our approach is expected to work best for the thermal quasi-equilibration time shorter than the polariton lifetime. We may find the regions of our phase diagram with optimal experimental accessibility as the quasi-equilibration time may depend on various physical parameters, *e.g.* R_s . One possible method for triggering our phase transitions may be the terahertz pump which has been shown to induce the s -wave to p -wave transition in the excitons [32].

Acknowledgement: We would like to thank Xi Dai, Hans Hansson, Joon Ik Jang, Na Young Kim, S. Raghu, Yao Wang and Fengcheng Wu for sharing their insights. S.B.C. acknowledges the hospitality of Nordita during its conference on “Multi-Component and Strongly Correlated Superconductors” where parts of this work has been completed. This research was supported by IBS-R009-Y1 (K.H.L. and S.B.C.) and Basic Science Research

Program through the National Research Foundation of Korea (NRF) funded by the Ministry of Education under Grant No. 2015R1D1A1A01058071 (C.L. and H.M.).

* hmin@snu.ac.kr

† chung.sukbum@gmail.com

- [1] B. Radisavljevic, A. Radenovic, J. Brivio, V. Giacometti, and A. Kis, *Nat. Nanotech.* **6**, 147 (2011).
- [2] D. Xiao, G.-B. Liu, W. Feng, X. Xu, and W. Yao, *Phys. Rev. Lett.* **108**, 196802 (2012).
- [3] N. F. Q. Yuan, K. F. Mak, and K. T. Law, *Phys. Rev. Lett.* **113**, 097001 (2014).
- [4] J. M. Lu, O. Zheliuk, I. Leermakers, N. F. Q. Yuan, U. Zeitler, K. T. Law, and J. T. Ye, *Science* **350**, 1353 (2015).
- [5] Y.-T. Hsu, A. Vaezi, M. H. Fischer, and E.-A. Kim, *Nat. Commun.* **8**, 14985 (2017).
- [6] D. Y. Qiu, F. H. da Jornada, and S. G. Louie, *Phys. Rev. Lett.* **111**, 216805 (2013).
- [7] M. M. Ugeda, A. J. Bradley, S.-F. Shi, F. H. da Jornada, Y. Zhang, D. Y. Qiu, W. Ruan, S.-K. Mo, Z. Hussain, Z.-X. Shen, F. Wang, S. G. Louie, and M. F. Crommie, *Nat. Mater.* **13**, 1091 (2014).
- [8] T. Cao, G. Wang, W. Han, H. Ye, C. Zhu, J. Shi, Q. Niu, P. Tan, E. Wang, B. Liu, and J. Feng, *Nat. Commun.* **3**, 887 (2012).
- [9] H. Zeng, J. Dai, W. Yao, D. Xiao, and X. Cui, *Nat. Nanotech.* **7**, 490 (2012).
- [10] K. F. Mak, C. Lee, J. Hone, J. Shan, and T. F. Heinz, *Phys. Rev. Lett.* **105**, 136805 (2010).
- [11] A. Splendiani, L. Sun, Y. Zhang, T. Li, J. Kim, C.-Y. Chim, G. Galli, and F. Wang, *Nano Lett.* **10**, 1271 (2010).
- [12] H. Deng, G. Weihs, C. Santori, J. Bloch, and Y. Yamamoto, *Science* **298**, 199 (2002).
- [13] J. Kasprzak, M. Richard, S. Kundermann, A. Baas, P. Jeambrun, J. M. J. Keeling, F. M. Marchetti, M. H. Szymańska, R. André, J. L. Staehli, V. Savona, P. B. Littlewood, B. Deveaud, and L. S. Dang, *Nature* **443**, 409 (2006).
- [14] R. Balili, V. Hartwell, D. Snoke, L. Pfeiffer, and K. West, *Science* **316**, 1007 (2007).
- [15] X. Liu, T. Galfsky, Z. Sun, F. Xia, E.-c. Lin, Y.-H. Lee, S. Kéna-Cohen, and V. M. Menon, *Nat. Photon.* **9**, 30 (2015).
- [16] Y.-J. Chen, J. D. Cain, T. K. Stanev, V. P. Dravid, and N. P. Stern, *Nat. Photon.* **11**, 431 (2017).
- [17] J. J. Baumberg, A. V. Kavokin, S. Christopoulos, A. J. D. Grundy, R. Butté, G. Christmann, D. D. Solnyshkov, G. Malpuech, G. Baldassarri Höger von Högersthal, E. Feltin, J.-F. Carlin, and N. Grandjean, *Phys. Rev. Lett.* **101**, 136409 (2008).
- [18] K. G. Lagoudakis, M. Wouters, M. Richard, A. Baas, I. Carusotto, R. Andre, L. S. Dang, and B. Deveaud-Pledran, *Nat Phys* **4**, 706 (2008).
- [19] S. Utsunomiya, L. Tian, G. Roumpos, C. W. Lai, N. Kumada, T. Fujisawa, M. Kuwata-Gonokami, A. Löffler, S. Hofling, A. Forchel, and Y. Yamamoto, *Nat Phys* **4**, 700 (2008).
- [20] A. Amo, J. Lefrere, S. Pigeon, C. Adrados, C. Ciuti, I. Carusotto, R. Houdre, E. Giacobino, and A. Bramati, *Nat Phys* **5**, 805 (2009).
- [21] F. M. Marchetti, J. Keeling, M. H. Szymańska, and P. B. Littlewood, *Phys. Rev. Lett.* **96**, 066405 (2006).
- [22] K. Kamide and T. Ogawa, *Phys. Rev. Lett.* **105**, 056401 (2010).
- [23] T. Byrnes, T. Horikiri, N. Ishida, and Y. Yamamoto, *Phys. Rev. Lett.* **105**, 186402 (2010).
- [24] J. P. Echeverry, B. Urbaszek, T. Amand, X. Marie, and I. C. Gerber, *Phys. Rev. B* **93**, 121107 (2016).
- [25] T. Byrnes, N. Y. Kim, and Y. Yamamoto, *Nat. Phys.* **10**, 803 (2014).
- [26] The no-photon ground state value in the Fock potential is subtracted off so that \hat{c}_k 's can be treated as the non-interacting quasiparticles with our band parameters.
- [27] Z. Ye, T. Cao, K. O'Brien, H. Zhu, X. Yin, Y. Wang, S. G. Louie, and X. Zhang, *Nature* **513**, 214 (2014).
- [28] L. Keldysh and Y. V. Kopayev, *Sov. Phys. Solid State* **6**, 2219 (1965).
- [29] M. J. Rice and S. Strässler, *Solid State Commun.* **13**, 1931 (1973).
- [30] F. D. M. Haldane, *Phys. Rev. Lett.* **61**, 2015 (1988).
- [31] The rotational symmetry breaking at two valleys are not independent due to the e-ph coupling. Therefore, if we take the \hat{H}_0 of Eq.(1), *i.e.* with the continuous rotational symmetry, we have for the two valley case the $SO(2)$ rather than $SO(2) \times SO(2)$ symmetry breaking. Given the photon polarization, the vanishing photon fraction is necessary for the rotational symmetry.
- [32] J. M. Ménard, C. Poellmann, M. Porer, U. Leierseder, E. Galopin, A. Lemaître, A. Amo, J. Bloch, and R. Huber, *Nat. Commun.* **5**, 4648 (2014).